

# Elastostatics of a Half-Plane under Random Boundary Excitations

Karl Sabelfeld · Irina Shalimova

Received: 29 March 2009 / Accepted: 23 October 2009 / Published online: 4 November 2009  
© Springer Science+Business Media, LLC 2009

**Abstract** A stochastic analysis of an elastostatics problem for a half-plane under random white noise excitations of the displacement vector prescribed on the boundary is given. Solutions of the problem are inhomogeneous random fields governed by the Lamé equation with random boundary conditions. This is used to model the displacements, strain tensor, vorticity, and the deformation energy, and to give exact representations for their correlation tensors, as well as the corresponding Karhunen-Loève (K-L) expansions. Numerical calculations illustrating the rate of convergence of the spectral and K-L expansions are also given. An interesting behaviour of the strain correlation tensor for the increasing value of the elasticity constant is found theoretically and confirmed by calculations. The paper presents the second part of our study, the first being published recently in Sabelfeld and Shalimova (J. Stat. Phys. 132(6):1071–1095, 2008) where only the displacement correlation tensor was derived and analyzed.

**Keywords** Lamé elasticity equation · Random displacement excitations · Karhunen-Loève expansions

## 1 Introduction

The problem of estimating the response to random excitations caused by different stochastically perturbed parameters of PDEs is of high interest in many fields of science and technology. The random excitations can be considered both as a natural source of stochastic

---

Support of the RFBR under Grants 09-01-00152-a, 09-01-12028-ofi-m, and 09-01-00639-a is kindly acknowledged.

---

K. Sabelfeld (✉) · I. Shalimova  
Institute of Computational Mathematics and Math. Geophysics, Russian Acad. Sci., Lavrentieva str., 6,  
630090 Novosibirsk, Russia  
e-mail: [karl@osmf.sccc.ru](mailto:karl@osmf.sccc.ru)

I. Shalimova  
e-mail: [ias@osmf.sccc.ru](mailto:ias@osmf.sccc.ru)

fluctuations, or as a model to describe extremely complicated irregularities and uncertainties (e.g., see [12, 19, 22]). We mention here such classical examples as the Navier-Stokes equation with a stochastic forcing, and the Darcy equation with a random hydraulic conductivity (e.g., see [1–3, 9]).

In electrical impedance tomography [6] important problem is to evaluate a global response to random boundary excitations, and to estimate local fluctuations of the solution fields. Similar analysis is made in the inverse problems of elastography [10, 15], recognition technology [4], acoustic scattering from rough surfaces [21], and reaction-diffusion equations with white noise boundary perturbations [19].

Unlike the fluctuations described by random coefficients of PDS, or their source terms, the random boundary conditions are not so well studied. The main reason is that in this case, we deal with *statistically inhomogeneous* random fields, hence the well known and commonly used spectral methods are here not applicable anymore. Another difficulty comes from the necessity to deal with boundary conditions and treat the relevant random boundary functions.

The main method for modeling inhomogeneous random fields is the Karhunen-Loève (K-L) expansion. Generally, it is computational demanding because it requires to solve numerically eigen-value problems of high dimension. However in some practically interesting cases models with analytically solvable eigen-value problem for the correlation operator can be obtained. This gives then a very efficient numerical method because as a rule, the K-L expansions are very fast convergent.

We deal in this paper with 2D zero mean random fields  $v(x, y)$  in a half-plane  $\{(x, y) : (-\infty < x < \infty, y > 0)\}$  which are homogeneous with respect to the longitudinal coordinate  $x$ , and inhomogeneous in the transverse direction  $y$ . Random fields with this property are called partially homogeneous [13]. The correlation function  $B_v = \langle v(x_1, y_1)v(x_2, y_2) \rangle$  is then depending on the difference  $\tau = x_1 - x_2$ . The partial spectral function is defined as the inverse Fourier transform with respect to  $\tau$ :

$$S_v(\xi, y_1, y_2) = F^{-1}[B_v](\xi, y_1, y_2) = \int_{-\infty}^{\infty} B_v(\tau, y_1, y_2)e^{-i\tau\xi} d\tau.$$

Assume we have no dependence on the variable  $y$ . The spectral representation of the random field is written in the form

$$v(x, \cdot) = \int_{\mathbb{R}} e^{i\xi x} G(\xi, \cdot)Z(d\xi) \tag{1}$$

where  $G$  is defined by  $G(\xi, \cdot)G^*(\xi, \cdot) = S(\xi, \cdot, \cdot)$ , the star sign stands for the complex conjugate, the sign  $\cdot$  stands to recall we omit the dependence on the variable  $y$ , and  $Z(d\xi)$  is a white noise on  $\mathbb{R}$ .

To simulate homogeneous random field, say,  $u(x)$ , one commonly uses the Randomized Spectral methods (e.g., see [7, 13, 18]) which is based on the randomized calculation of the stochastic integral (1). Another method is based on the Riemann sums calculation with fixed cells. The integral is approximated by a finite sum

$$u(x) \approx \sum_{i=1}^N [\zeta_i \sin(\xi_i x) + \eta_i \cos(\xi_i x)]$$

where  $\xi_i$  are deterministic nodes in the Fourier space,  $\zeta_i$  and  $\eta_i$  are Gaussian variables with zero mean and relevant covariance.

In our case we have however the dependence on the variable  $y$ , and the random fields are partially inhomogeneous. In [13] we have extended the Spectral Randomization method to general partially homogeneous random fields, but the inhomogeneity in  $y$  was still a problem assumed to be solved by other methods. In a sense it was a method which reduced the dimension of the problem (see for details [13]).

In the case we deal with, the partial spectral function has a special structure, namely,  $S(\xi, y_1, y_2)$  depends on  $y_1$  and  $y_2$  as follows:  $S(\xi, y_1, y_2) = G(\xi, y_1)G^*(\xi, y_2)$ . This enables to construct a simple extension of the Randomization method, without solving the inhomogeneity problem in  $y$ , see [14] and [17]. This was first done in [14] by using the Karhunen-Loève expansion.

Assume now, without loss of generality, that a generally inhomogeneous random field  $u(x)$  has a zero mean and a variance  $E u^2(x)$  that is bounded. The Karhunen-Loève expansion has the form [23]

$$u(x) = \sum_{k=1}^{\infty} \sqrt{\lambda_k} \zeta_k h_k(x),$$

where  $\lambda_k$  and  $h_k(x)$  are the eigen-values and eigen-functions of the correlation function  $B(x_1, x_2) = \langle u(x_1)u(x_2) \rangle$ , and  $\zeta_k$  is a family of random variables.

By definition,  $B(x_1, x_2)$  is bounded, symmetric and positive definite. For such kernels, the Hilbert-Schmidt theory says that the following spectral representation is valid

$$B(x_1, x_2) = \sum_{k=1}^{\infty} \lambda_k h_k(x_1)h_k(x_2)$$

where the eigen-values and eigen-functions are the solutions of the following eigen-value problem for the correlation operator:

$$\int B(x_1, x_2)h_k(x_1)dx_1 = \lambda_k h_k(x_2).$$

The eigen-functions form a complete orthogonal set  $\int h_i(x)h_j(x) dx = \delta_{ij}$  where  $\delta_{ij}$  is the Kronecker delta-function. The family  $\{\zeta_k\}$  is a set of uncorrelated random variables which are obviously related to  $h_k$  by

$$\zeta_k = \frac{1}{\sqrt{\lambda_k}} \int u(x)h_k(x) dx, \quad E \zeta_k = 0, \quad E \zeta_i \zeta_j = \delta_{ij}.$$

It is well known that the Karhunen-Loève expansion presents an optimal (in the mean square sense) convergence for any distribution of  $u(x)$ . If  $u(x)$  is a zero mean Gaussian random field, then  $\{\zeta_k\}$  is a family of standard Gaussian random variables. We assume in this study that the random fields are Gaussian. Some generalizations to non-Gaussian random fields are reported in [11].

Consider now a case when the domain is unbounded, e.g., a homogeneous random process  $u(x)$  is defined on the whole real line  $\mathbb{R}$ . The eigen-value problem reads

$$\int_{\mathbb{R}} B(x_2 - x_1)h_k(x_1) dx_1 = \lambda_k h_k(x_2), \quad -\infty < x_2 < \infty. \tag{2}$$

Note that we can take  $h(x) = e^{i\omega x}$ , then from (2) we get

$$\lambda = \int_{-\infty}^{\infty} B(x_2 - x_1)e^{-i\omega(x_2-x_1)} dx_1 \equiv S(\omega).$$

To make further considerations more rigorous, we assume that our domain is bounded, say,  $-a \leq x \leq a$ , and  $u$  is periodic (e.g., see [8, 20]). Then, we may develop  $B(x_2 - x_1)$  in a Fourier series,

$$B(x - x') = \sum_k \lambda_k e^{i2\pi k(x-x')}. \tag{3}$$

The eigen-value problem can then be solved via the unique representation

$$B(x - x') = \sum_k \lambda_k e^{i2\pi kx} e^{-i2\pi kx'} \tag{4}$$

which imply that  $e^{i2\pi kx}$  are the eigen-functions with eigen-values  $\lambda_k = S(\omega_k)$ . And conversely, if the eigen-functions are Fourier modes we can write the equality (4) which leads to (3).

We apply the cut-off in the integration, i.e., we have to solve the eigen-value problem

$$\int_{-a}^a B(x_2 - x_1)h(x_1) dx_1 = \lambda_k h_k(x_2),$$

where  $a$  is sufficiently large. Then it is possible to show (e.g., see [20]) that

$$\lambda_k \approx S(\omega_k) = S(\pi k/a), \quad h_k(x) \approx \frac{1}{2\pi} e^{i(\pi kx/a)},$$

which yields an approximation

$$B(x_1, x_2) \approx \tilde{B}_a(x_1, x_2) = \sum_{k=1}^{\infty} \frac{1}{a} S\left(\frac{\pi k}{a}\right) \cos\left(\frac{\pi k(x_2 - x_1)}{a}\right),$$

and the K-L expansion approaches in this case to the spectral representation

$$u(x) \approx \tilde{u}_a(x) = \sum_{k=1}^{\infty} \left[ \frac{1}{a} S\left(\frac{\pi k}{a}\right) \right]^{1/2} \left\{ \zeta_k \cos[\pi kx/a] + \eta_k \sin[\pi kx/a] \right\}.$$

The rate of convergence of the K-L expansion is closely related to the smoothness of the correlation kernel and to ratio between the length  $a$  and  $L$ , the correlation length of the process. For example, in [8] is reported that for the particular case  $B(x_1, x_2) = \sigma e^{-|x_2-x_1|/L}$ , an upper bound for the relative error in variance  $\varepsilon$  of the process represented by its K-L expansion is given by  $\varepsilon \leq \frac{4}{\pi^2} \frac{1}{n} \frac{a}{L}$  where  $n$  is the number of retained terms.

In this paper we give exact K-L expansions of the solution and its derivatives for an elastostatics of a 2D elastic half-plane with random displacements prescribed on the boundary. The problem is governed by a system of Lamé equations with random Dirichlet boundary conditions. This paper continues the study we have published recently in [17] and [14] which

deals with random boundary value problems for a disc and a half-plane. The main contribution of the present paper is the derivation of the correlation functions and the Karhunen-Loève expansions for different tensors like the stress and vorticity, as well as the exact representation for the mean elastic energy.

## 2 Elastostatics Equations and the Poisson Formula for the Half-Plane

Let us consider the Dirichlet problem for the system of Lamé equations in the domain  $D^+ \subset \mathbb{R}^2$ , the upper half-plane with the boundary  $\Gamma = \{(x, y) : y = 0\}$ :

$$\Delta \mathbf{u}(\mathbf{x}) + \alpha \operatorname{grad} \operatorname{div} \mathbf{u}(\mathbf{x}) = 0, \quad \mathbf{x} \in D^+, \quad \mathbf{u}(x') = \mathbf{g}(x') \quad x' \in \Gamma = \partial D^+, \quad (5)$$

where  $\mathbf{u}(\mathbf{x}) = (u_1(x, y), u_2(x, y))^T$  is a column vector of displacements, and  $\mathbf{g} = (g_1, g_2)^T$  is the vector of displacements prescribed on the boundary. The elastic constant  $\alpha = \frac{\lambda + \mu}{\mu}$  is expressed through the Lamé constants of elasticity  $\lambda$  and  $\mu$ .

The Poisson formula for the problem (5) has the form [17]

$$\mathbf{u}(x, y) = \int_{-\infty}^{\infty} P(x - x', y) \mathbf{g}(x') dx', \quad (6)$$

where  $P(x - x', y) = K(x - x', y)Q(x - x', y)$  is defined via

$$K(x - x', y) = \frac{y}{\pi((x - x')^2 + y^2)},$$

the kernel of the well-known Poisson formula for the Dirichlet problem for the Laplace equation in the half-plane, (e.g., see [14, 17]), and

$$Q(x - x', y) = \mathbf{I} + \frac{\beta}{(x - x')^2 + y^2} \begin{pmatrix} (x - x')^2 - y^2 & 2(x - x')y \\ 2(x - x')y & -((x - x')^2 - y^2) \end{pmatrix}, \quad (7)$$

where  $\mathbf{I}$  is the identity matrix, and  $\beta = \frac{\lambda + \mu}{\lambda + 3\mu}$ .

## 3 Stochastic Boundary Value Problem

### 3.1 Correlation Tensor of the Displacements

Assume the prescribed boundary displacements  $g_i, i = 1, 2$  in (5) are homogeneous random processes defined on the whole line  $\mathbb{R}$ . Then, the solution  $\mathbf{u}(x, y)$  of the problem (5) is a random field, and our goal is to find its main statistical characteristics, e.g., the correlation tensor of the displacements and strain, and the mean elastic energy. Here we note that from the Poisson formula (6) it can be easily found that  $\langle \mathbf{u} \rangle = \langle \mathbf{g} \rangle$ , so without loss of generality we assume that  $\langle \mathbf{g} \rangle = 0$ . For simplicity, we deal here with Gaussian random fields, so we suppose that  $g_i$  are Gaussian random processes, which implies due to (6) that  $\mathbf{u}(x, y)$  is also a Gaussian random field. Then, this zero mean random field is uniquely defined by its correlation tensor.

From the Poisson formula (6) for  $\mathbf{u}$ , the correlation tensor  $B_u(x_1, y_1; x_2, y_2)$  for the displacements can be written as follows

$$\begin{aligned}
 B_u(x_1, y_1; x_2, y_2) &= \langle \mathbf{u}(x_1, y_1) \otimes \mathbf{u}(x_2, y_2) \rangle = \langle \mathbf{u}(x_1, y_1) \mathbf{u}^T(x_2, y_2) \rangle \\
 &= \int_{-\infty}^{\infty} \int_{-\infty}^{\infty} P(x_1 - x'_1, y_1) B_g(x'_1; x'_2) P^T(x_2 - x'_2, y_2) dx'_1 dx'_2. \quad (8)
 \end{aligned}$$

We use here the notation  $\otimes$  for the direct product of vectors  $\mathbf{u}(x_1, y_1)$  and  $\mathbf{u}(x_2, y_2)$ , and  $B_g(x_1; x_2)$  for the correlation tensor of the random boundary vector  $\mathbf{g}$

$$B_g(x'_1; x'_2) = \langle \mathbf{g}(x'_1) \otimes \mathbf{g}(x'_2) \rangle.$$

We deal in this paper with the case when  $\mathbf{g}$  is a Gaussian white noise. This implies that

$$\{B_g(x'_1; x'_2)\}_{ij} = \delta_{ij} \delta(x'_1 - x'_2), \quad i, j = 1, 2.$$

Here we use standard notations,  $\delta_{ij}$  for the Kronecker symbol, and  $\delta(x'_1 - x'_2)$  for the Dirac  $\delta$ -function. In this case, (8) simplifies to

$$B_u(x_1, y_1; x_2, y_2) = \int_{-\infty}^{\infty} P(x_1 - x'_1, y_1) P(x_2 - x'_1, y_2) dx'_1$$

where we used the fact that  $P = P^T$ . To integrate the right-hand side we use the Fourier transformation, so we rewrite the last equality in the form of a convolution. The change of variables  $z = x_1 - x'_1$  yields

$$B_u(x_1, y_1; x_2, y_2) = \int_{-\infty}^{\infty} P(z, y_1) P_1(x_1 - x_2 - z, y_2) dz = P(\cdot, y_1) * P_1(\cdot, y_2), \quad (9)$$

where the matrix kernel  $P_1$  is defined by  $P_1(z, y) = P(-z, y)$ .

Thus (9) has the form of convolution, and we can use the Fourier property for convolutions. Note that  $B_u(x_1, y_1; x_2, y_2)$  depends on the difference,  $\tau = x_1 - x_2$ , so we will write  $B_u(\tau, y_1, y_2)$  instead of  $B_u(x_1, x_2; y_1, y_2)$ .

The Fourier transform property for convolutions yields

$$F^{-1}[B_u] = F^{-1}[P(z, y_1)] F^{-1}[P_1(x_1 - x_2 - z, y_2)].$$

So we have to find the inverse transforms  $F^{-1}[P(\cdot, y_1)]$  and  $F^{-1}[P_1(\cdot, y_2)]$ .

Notice that  $F^{-1}[P_1(x_1 - x_2 - z, y)](\xi, y) = F^{-1}[P(z, y)](-\xi, y)$ , so using the Fourier transform formulae given in the Appendix, (see also [5]), we get

$$F^{-1}[B_u] = e^{-|\xi|(y_1+y_2)} \left( \mathbf{I} - \beta y_1 \begin{pmatrix} |\xi| & i\xi \\ i\xi & -|\xi| \end{pmatrix} \right) \left( \mathbf{I} - \beta y_2 \begin{pmatrix} |\xi| & -i\xi \\ -i\xi & -|\xi| \end{pmatrix} \right). \quad (10)$$

The correlation tensor  $B_u$  is now obtained by converting these equalities by the relevant Fourier transforms. Indeed, using the Fourier transform formulae (see Appendix) we finally

get the desired representation for the tensor  $B_u$

$$\begin{aligned}
 & B_u(\tau, y_1, y_2) \\
 &= \frac{y_1 + y_2}{\pi(\tau^2 + (y_1 + y_2)^2)} \mathbf{I} \\
 &+ \frac{\beta(y_1 + y_2)}{\pi(\tau^2 + (y_1 + y_2)^2)^2} \begin{pmatrix} \tau^2 - (y_1 + y_2)^2 & 2\tau(y_1 - y_2) \\ 2\tau(y_1 - y_2) & -(\tau^2 - (y_1 + y_2)^2) \end{pmatrix} \\
 &+ \frac{4y_1y_2\beta^2}{\pi(\tau^2 + (y_1 + y_2)^2)^3} \begin{pmatrix} (y_1 + y_2)((y_1 + y_2)^2 - 3\tau^2) & \tau(3(y_1 + y_2)^2 - \tau^2) \\ -\tau(3(y_1 + y_2)^2 - \tau^2) & (y_1 + y_2)((y_1 + y_2)^2 - 3\tau^2) \end{pmatrix}. \tag{11}
 \end{aligned}$$

### 3.2 Correlation Function of the Vorticity

Using the Poisson formula (6), we can analogously derive the correlation function for the vorticity  $w(x, y)$  which is defined by

$$w(x, y) = \frac{\partial u_1(x, y)}{\partial y} - \frac{\partial u_2(x, y)}{\partial x}.$$

Indeed, by definition,

$$\begin{aligned}
 B_w(x_1, y_1; x_2, y_2) &= \langle w(x_1, y_1)w(x_2, y_2) \rangle \\
 &= \left\langle \left( \frac{\partial u_1}{\partial y}(x_1, y_1) - \frac{\partial u_2}{\partial x}(x_1, y_1) \right) \left( \frac{\partial u_1}{\partial y}(x_2, y_2) - \frac{\partial u_2}{\partial x}(x_2, y_2) \right) \right\rangle.
 \end{aligned}$$

By the Poisson formula (6)

$$\begin{aligned}
 & B_w(x_1, y_1; x_2, y_2) \\
 &= \left\langle \int_{-\infty}^{\infty} \left( \frac{\partial P_{11}}{\partial y} - \frac{\partial P_{21}}{\partial x} \right) (x_1 - x', y_1) g_1(x') + \left( \frac{\partial P_{12}}{\partial y} - \frac{\partial P_{22}}{\partial x} \right) (x_1 - x', y_1) g_2(x') dx' \right. \\
 &\quad \times \int_{-\infty}^{\infty} \left( \frac{\partial P_{11}}{\partial y} - \frac{\partial P_{21}}{\partial x} \right) (x_1 - x'', y_2) g_1(x'') \\
 &\quad \left. + \left( \frac{\partial P_{12}}{\partial y} - \frac{\partial P_{22}}{\partial x} \right) (x_1 - x'', y_2) g_2(x'') dx'' \right\rangle.
 \end{aligned}$$

For  $g_i$  is a white noise, we get

$$\begin{aligned}
 B_w &= \int_{-\infty}^{\infty} \left( \frac{\partial P_{11}}{\partial y} - \frac{\partial P_{21}}{\partial x} \right) (x_1 - x', y_1) \left( \frac{\partial P_{11}}{\partial y} - \frac{\partial P_{21}}{\partial x} \right) (x_2 - x', y_2) dx' \\
 &\quad + \int_{-\infty}^{\infty} \left( \frac{\partial P_{12}}{\partial y} - \frac{\partial P_{22}}{\partial x} \right) (x_1 - x', y_1) \left( \frac{\partial P_{12}}{\partial y} - \frac{\partial P_{22}}{\partial x} \right) (x_2 - x', y_2) dx'. \tag{12}
 \end{aligned}$$

By the change of integration variable  $x'$  to  $z = x_1 - x'$ , and recalling that  $\tau = x_1 - x_2$ , we rewrite (12) in a convolution form,

$$B_w(\tau, y_1, y_2) = \left(\frac{\partial P_{11}}{\partial y} - \frac{\partial P_{21}}{\partial x}\right)(z, y_1) * \left(\frac{\partial P_{11}}{\partial y} - \frac{\partial P_{21}}{\partial x}\right)_-(\tau - z, y_2) + \left(\frac{\partial P_{12}}{\partial y} - \frac{\partial P_{22}}{\partial x}\right)(z, y_1) * \left(\frac{\partial P_{12}}{\partial y} - \frac{\partial P_{22}}{\partial x}\right)_-(\tau - z, y_2)$$

where we use the notation  $(G(x, y))_-$  meaning that a function  $G$  is taken at  $-x$ , i.e.,  $(G(x, y))_- = G(-x, y)$ .

Applying now the Fourier transform with respect to the variable  $\tau$ , and using the Fourier transform property for convolutions we get

$$F^{-1}[B_w](\xi, y_1, y_2) = F^{-1}\left[\left(\frac{\partial P_{11}}{\partial y} - \frac{\partial P_{21}}{\partial x}\right)(\cdot, y_1)\right]F^{-1}\left[\left(\frac{\partial P_{11}}{\partial y} - \frac{\partial P_{21}}{\partial x}\right)_-(\cdot, y_2)\right] + F^{-1}\left[\left(\frac{\partial P_{12}}{\partial y} - \frac{\partial P_{22}}{\partial x}\right)(\cdot, y_1)\right]F^{-1}\left[\left(\frac{\partial P_{12}}{\partial y} - \frac{\partial P_{22}}{\partial x}\right)_-(\cdot, y_2)\right]. \tag{13}$$

To write down it in a more compact form, we introduce the notation:

$$G_1(\cdot, y) = \left(\frac{\partial P_{11}}{\partial y} - \frac{\partial P_{21}}{\partial x}\right)(\cdot, y), \quad G_2(\cdot, y) = \left(\frac{\partial P_{12}}{\partial y} - \frac{\partial P_{22}}{\partial x}\right)(\cdot, y). \tag{14}$$

Then, we get from (13):

$$F^{-1}[B_w](\xi, y_1, y_2) = F^{-1}[G_1](\xi, y_1) \cdot F^{-1}[G_1](-\xi, y_2) + F^{-1}[G_2](\xi, y_1) \cdot F^{-1}[G_2](-\xi, y_2). \tag{15}$$

To find the Fourier transforms of  $G_1$  and  $G_2$ , we turn from the derivatives with respect to  $x$  to the derivatives with respect to  $\tau$ , so that we can use directly the Fourier transform formulae given in the Appendix. This yields

$$F^{-1}[B_w] = 2(1 + \beta)^2 \xi^2 e^{-|\xi|(y_1+y_2)}. \tag{16}$$

Converting the Fourier transform we obtain the exact representation for the vorticity correlation function

$$B_w = 4(1 + \beta)^2 (y_1 + y_2) \frac{(y_1 + y_2)^2 - 3\tau^2}{\pi(\tau^2 + (y_1 + y_2)^2)^3}.$$

### 3.3 Correlation Functions of the Strain

By definition  $\varepsilon_{ij}(x, y)$  is

$$\varepsilon_{11}(x, y) = \frac{\partial u_1(x, y)}{\partial x}, \quad \varepsilon_{22}(x, y) = \frac{\partial u_2(x, y)}{\partial y},$$

and

$$\varepsilon_{12}(x, y) = \varepsilon_{21}(x, y) = \frac{1}{2} \left( \frac{\partial u_1(x, y)}{\partial y} + \frac{\partial u_2(x, y)}{\partial x} \right).$$



The correlation  $B_{\varepsilon_{11}}$  is

$$B_{\varepsilon_{11}}(x_1, y_1; x_2, y_2) = \langle \varepsilon_{11}(x_1, y_1) \varepsilon_{11}(x_2, y_2) \rangle.$$

Further steps are quite analogous to that of the evaluation of the vorticity correlation function we have presented above in Sect. 3.2. Indeed, we have the convolution representation

$$B_{\varepsilon_{11}}(\tau, y_1, y_2) = \int_{-\infty}^{\infty} \frac{\partial P_{11}}{\partial x}(z, y_1) \left( \frac{\partial P_{11}}{\partial x} \right)_-(\tau - z, y_2) dz + \int_{-\infty}^{\infty} \frac{\partial P_{12}}{\partial x}(z, y_1) \left( \frac{\partial P_{12}}{\partial x} \right)_-(\tau - z, y_2) dz.$$

To take the Fourier transform of both sides of this convolution, we just notice that the result will coincide with (15) if the functions  $G_1$  and  $G_2$  in (14) are substituted by  $G_1(\cdot, y) = \frac{\partial P_{11}}{\partial x}(\cdot, y)$  and  $G_2(\cdot, y) = \frac{\partial P_{12}}{\partial x}(\cdot, y)$ , respectively. So we can use the formula (15) with these functions  $G_1$  and  $G_2$ , which after some calculations with the help of Fourier formulae given in the Appendix yields

$$F^{-1}[B_{\varepsilon_{11}}] = \xi^2 e^{-|\xi|(y_1+y_2)} \left[ 1 - \beta|\xi|(y_1 + y_2) + 2\beta^2 y_1 y_2 \xi^2 \right]. \tag{17}$$

The inverse Fourier transform results in the exact representation

$$B_{\varepsilon_{11}} = 2(y_1 + y_2) \left[ \frac{((y_1 + y_2)^2 - 3\tau^2)}{\pi(\tau^2 + (y_1 + y_2)^2)^3} - 3\beta \frac{(y_1 + y_2)^4 + \tau^4 - 6(y_1 + y_2)^2 \tau^2}{\pi(\tau^2 + (y_1 + y_2)^2)^4} + 24\beta^2 y_1 y_2 \frac{(y_1 + y_2)^4 + 5\tau^4 - 10(y_1 + y_2)^2 \tau^2}{\pi(\tau^2 + (y_1 + y_2)^2)^5} \right].$$

The case of  $B_{\varepsilon_{22}}$  is treated exactly the same, we just have to substitute  $G_1(\cdot, y) = \frac{\partial P_{21}}{\partial x}(\cdot, y)$  and  $G_2(\cdot, y) = \frac{\partial P_{22}}{\partial x}(\cdot, y)$ , respectively. So it remains only to calculate the relevant Fourier transforms which is done by the use of Fourier transform formulae of the Appendix

$$F^{-1}[B_{\varepsilon_{22}}] = \xi^2 e^{-|\xi|(y_1+y_2)} \left[ \beta^2 + (1 - \beta)^2 + (\beta - 2\beta^2)(y_1 + y_2)|\xi| + 2\beta^2 y_1 y_2 \xi^2 \right], \tag{18}$$

and to take the Fourier inverse:

$$B_{\varepsilon_{22}} = 2(y_1 + y_2) \left[ (\beta^2 + (1 - \beta)^2) \frac{(y_1 + y_2)^2 - 3\tau^2}{\pi(\tau^2 + (y_1 + y_2)^2)^3} + 3(\beta - 2\beta^2) \frac{(y_1 + y_2)^4 + \tau^4 - 6(y_1 + y_2)^2 \tau^2}{\pi(\tau^2 + (y_1 + y_2)^2)^4} + 24\beta^2 y_1 y_2 \frac{(y_1 + y_2)^4 + 5\tau^4 - 10(y_1 + y_2)^2 \tau^2}{\pi(\tau^2 + (y_1 + y_2)^2)^5} \right].$$

Since the calculations of  $B_{\varepsilon_{12}}$  are very similar, especially to the derivation of vorticity correlation function, we simply present the final result:

$$F^{-1}[B_{\varepsilon_{12}}] = \frac{1}{2} \xi^2 e^{-|\xi|(y_1+y_2)} \left[ 1 + \beta^2 + 4\beta^2 y_1 y_2 \xi^2 - \beta^2 |\xi| (y_1 + y_2) \right]. \tag{19}$$

Hence,

$$B_{\varepsilon_{12}} = (y_1 + y_2) \left[ (1 + \beta^2) \frac{(y_1 + y_2)^2 - 3\tau^2}{\pi(\tau^2 + (y_1 + y_2)^2)^3} - 6\beta^2 \frac{(y_1 + y_2)^4 + \tau^4 - 6(y_1 + y_2)^2 \tau^2}{\pi(\tau^2 + (y_1 + y_2)^2)^4} + 48\beta^2 y_1 y_2 \frac{(y_1 + y_2)^4 + 5\tau^4 - 10(y_1 + y_2)^2 \tau^2}{\pi(\tau^2 + (y_1 + y_2)^2)^5} \right].$$

### 3.4 The Mean Deformation Energy

Let us consider the mean deformation energy  $\langle E(x, y) \rangle$  defined by

$$\langle E(x, y) \rangle = \left\langle \frac{\lambda}{2} (\varepsilon_{11} + \varepsilon_{22})^2 + \mu \sum_{i,j} \varepsilon_{ij}^2 \right\rangle.$$

Using the Poisson formula (6), we obtain

$$\begin{aligned} \langle E(x, y) \rangle &= \frac{\lambda}{2} \int_{-\infty}^{\infty} \left( \frac{\partial P_{11}}{\partial x} + \frac{\partial P_{21}}{\partial y} \right)^2 + \left( \frac{\partial P_{12}}{\partial x} + \frac{\partial P_{22}}{\partial y} \right)^2 \Big|_{(x-x',y)} dx' \\ &\quad + \mu \int_{-\infty}^{\infty} \left( \frac{\partial P_{11}}{\partial x} \right)^2 + \left( \frac{\partial P_{12}}{\partial x} \right)^2 + \left( \frac{\partial P_{21}}{\partial y} \right)^2 + \left( \frac{\partial P_{22}}{\partial y} \right)^2 \Big|_{(x-x',y)} dx' \\ &\quad + \frac{\mu}{2} \int_{-\infty}^{\infty} \left( \frac{\partial P_{11}}{\partial y} + \frac{\partial P_{21}}{\partial x} \right)^2 + \left( \frac{\partial P_{12}}{\partial y} + \frac{\partial P_{22}}{\partial x} \right)^2 \Big|_{(x-x',y)} dx'. \end{aligned}$$

After some algebra we arrive at

$$\langle E(x, y) \rangle = \frac{2\mu(\lambda + 2\mu)}{\pi^2(\lambda + 3\mu)} \int_{-\infty}^{\infty} \frac{dx'}{((x - x')^2 + y^2)^2} + \frac{8\mu(\lambda + \mu)^2 y^2}{\pi^2(\lambda + 3\mu)^2} \int_{-\infty}^{\infty} \frac{dx'}{((x - x')^2 + y^2)^3},$$

which can be evaluated explicitly

$$\langle E(x, y) \rangle = \frac{\mu}{\pi y^3} \left( \frac{\lambda + 2\mu}{\lambda + 3\mu} + \frac{(\lambda + \mu)^2}{(\lambda + 3\mu)^2} \right).$$

## 4 Karhunen-Loève Expansions and Simulation Algorithm

As seen from the previous section, exact results can be obtained for the correlation functions of vorticity, strain, and some other functions like the mean elastic energy. For more

complicated statistical characteristics this would be impossible. Therefore, it is very important to construct simulation formulae for the random fields itself, say for the displacements, strain and stress tensors. In [17], we have constructed the Karhunen-Loève expansions for the displacements. We will use these expansions to construct the relevant expansions for the vorticity, strains, and the elastic energy.

The K-L expansion for the displacement vector  $\mathbf{u}(x, y)$  has the form [17]:

$$\begin{pmatrix} u_1(x, y) \\ u_2(x, y) \end{pmatrix} \approx \frac{1}{\sqrt{R}} \sum_{k=1}^n e^{-\frac{\pi k}{R} y} \left[ \begin{pmatrix} (1 - \beta \frac{\pi k}{R} y)(\zeta_k \cos[\pi kx/R] + \tilde{\zeta}_k \sin[\pi kx/R]) \\ \beta \frac{\pi k}{R} y(\zeta_k \sin[\pi kx/R] - \tilde{\zeta}_k \cos[\pi kx/R]) \end{pmatrix} - \begin{pmatrix} \beta \frac{\pi k}{R} y(\eta_k \cos[\pi kx/R] + \tilde{\eta}_k \sin[\pi kx/R]) \\ -(1 + \beta \frac{\pi k}{R} y)(\eta_k \sin[\pi kx/R] - \tilde{\eta}_k \cos[\pi kx/R]) \end{pmatrix} \right] \tag{20}$$

where  $\zeta_k$  and  $\eta_k$  are independent Gaussian random variables such that

$$\langle \zeta_k \zeta_j \rangle = \delta_{jk}, \quad \langle \eta_k \eta_j \rangle = \delta_{jk}, \quad \langle \eta_k \rangle = 0, \quad \langle \zeta_k \rangle = 0,$$

and the same for the family  $\{\tilde{\zeta}_k, \tilde{\eta}_k\}$  which is independent of  $\{\zeta_k, \eta_k\}$ . As mentioned in the Introduction, the rate of convergence of this kind of approximations, as  $R \rightarrow \infty$ , is proportional to  $R/nL$  where  $n$  is the number of terms, and  $L$  is a characteristic correlation length of the random field. For brevity, we will write in what follows the equality sign “=” instead of “ $\approx$ ” which is understood in the same sense as (20).

Taking the derivatives termwise in (20) we get the desired expansions for the strain tensor and vorticity:

$$\begin{aligned} \varepsilon_{11}(x, y) = & \frac{1}{\sqrt{R}} \sum_{k=1}^{\infty} \frac{\pi k}{R} e^{-\frac{\pi k}{R} y} \left[ \left( (-1 + \beta \frac{\pi k}{R} y) \zeta_k + \beta \frac{\pi k}{R} y \eta_k \right) \sin \frac{\pi kx}{R} \right. \\ & \left. + \left( (1 - \beta \frac{\pi k}{R} y) \tilde{\zeta}_k + \beta \frac{\pi k}{R} y \tilde{\eta}_k \right) \cos \frac{\pi kx}{R} \right], \end{aligned} \tag{21}$$

$$\begin{aligned} \varepsilon_{22}(x, y) = & \frac{1}{\sqrt{R}} \sum_{k=1}^{\infty} \frac{\pi k}{R} e^{-\frac{\pi k}{R} y} \left[ \left( (1 - \frac{\pi k}{R} y) \beta \zeta_k + \left( \beta - 1 - \beta \frac{\pi k}{R} y \right) \eta_k \right) \sin \frac{\pi kx}{R} \right. \\ & \left. + \left( (-1 + \frac{\pi k}{R} y) \beta \tilde{\zeta}_k + \left( \beta - 1 - \beta \frac{\pi k}{R} y \right) \tilde{\eta}_k \right) \cos \frac{\pi kx}{R} \right], \end{aligned} \tag{22}$$

$$\begin{aligned} \varepsilon_{12}(x, y) = & \frac{1}{2\sqrt{R}} \sum_{k=1}^{\infty} \frac{\pi k}{R} e^{-\frac{\pi k}{R} y} \left[ \left( (-1 - \beta + 2\beta \frac{\pi k}{R} y) \tilde{\zeta}_k \right. \right. \\ & \left. + \left( \beta - 1 - 2\beta \frac{\pi k}{R} y \right) \tilde{\eta}_k \right) \sin \frac{\pi kx}{R} \\ & \left. + \left( (-1 - \beta + 2\beta \frac{\pi k}{R} y) \zeta_k + \left( 1 - \beta + 2\beta \frac{\pi k}{R} y \right) \eta_k \right) \cos \frac{\pi kx}{R} \right], \end{aligned} \tag{23}$$

$$w(x, y) = (\beta + 1) \frac{\sqrt{2}}{\sqrt{R}} \sum_{k=1}^{\infty} \frac{\pi k}{R} e^{-\frac{\pi k}{R} y} \left[ \zeta_k \sin \frac{\pi kx}{R} + \eta_k \cos \frac{\pi kx}{R} \right]. \tag{24}$$

It should be noted that the random fields given by the K-L expansions (21)–(24) all have the following structure: they consist of two independent random fields, say,  $V_1$  and  $V_2$ , whose partial spectral functions are  $F^{-1}[G_1](\xi, y_1)F^{-1}[G_1](-\xi, y_2)$ , and  $F^{-1}[G_2](\xi, y_1)F^{-1}[G_2](-\xi, y_2)$ , respectively, where  $G_1$  and  $G_2$  are defined as described above (e.g., in the case of vorticity, see (14)). This follows directly from the formula (15). Indeed, let us present this in more details which by the way will simplify the simulation formulae (21)–(24).

Let us introduce the notation for the “discrete wave number” by  $\xi_k = \frac{\pi k}{R}$ . We split the expansions (21)–(24) in the form  $\varepsilon_{ij} = V_1 + V_2$  where  $V_1, V_2$  are independent random fields. Then, using the symmetry property of the Gaussian distribution we obtain for (21),

$$\begin{aligned}
 V_1(x, y) &= \frac{1}{\sqrt{R}} \sum_{k=1}^{\infty} \xi_k e^{-\xi_k y} (1 - \beta \xi_k y) \left[ \zeta_k \sin(\xi_k x) + \tilde{\zeta}_k \cos(\xi_k x) \right], \\
 V_2(x, y) &= \frac{\beta y}{\sqrt{R}} \sum_{k=1}^{\infty} \xi_k^2 e^{-\xi_k y} \left[ \eta_k \sin(\xi_k x) + \tilde{\eta}_k \cos(\xi_k x) \right].
 \end{aligned}
 \tag{25}$$

From these representations, it is clearly seen by comparing with (17) that the random field  $\varepsilon_{11} = V_1 + V_2$  has the desired spectral function.

Similar calculations give, for  $\varepsilon_{22} = V_1 + V_2$ :

$$\begin{aligned}
 V_1(x, y) &= \frac{\beta}{\sqrt{R}} \sum_{k=1}^{\infty} \xi_k e^{-\xi_k y} (1 - \xi_k y) \left[ \zeta_k \sin(\xi_k x) + \tilde{\zeta}_k \cos(\xi_k x) \right], \\
 V_2(x, y) &= \frac{1}{\sqrt{R}} \sum_{k=1}^{\infty} \xi_k e^{-\xi_k y} (1 - \beta + \beta \xi_k y) \left[ \eta_k \sin(\xi_k x) + \tilde{\eta}_k \cos(\xi_k x) \right],
 \end{aligned}
 \tag{26}$$

for  $\varepsilon_{12} = V_1 + V_2$ :

$$\begin{aligned}
 V_1(x, y) &= \frac{1}{2\sqrt{R}} \sum_{k=1}^{\infty} \xi_k e^{-\xi_k y} (1 + \beta - 2\beta \xi_k y) \left[ \zeta_k \sin(\xi_k x) + \tilde{\zeta}_k \cos(\xi_k x) \right], \\
 V_2(x, y) &= \frac{1}{2\sqrt{R}} \sum_{k=1}^{\infty} \xi_k e^{-\xi_k y} (1 - \beta + 2\beta \xi_k y) \left[ \eta_k \sin(\xi_k x) + \tilde{\eta}_k \cos(\xi_k x) \right],
 \end{aligned}
 \tag{27}$$

and for the vorticity,

$$w(x, y) = (\beta + 1) \frac{\sqrt{2}}{\sqrt{R}} \sum_{k=1}^{\infty} \xi_k e^{-\xi_k y} \left[ \zeta_k \sin(\xi_k x) + \tilde{\zeta}_k \cos(\xi_k x) \right].
 \tag{28}$$

From these representations it follows that  $V_1$  and  $V_2$  are the Karhunen-Loève expansions over the eigen-functions which solve the eigen-value problem for the relevant correlation functions having the corresponding partial spectral functions.

We use these expansions in numerical simulations presented in the next section.

### 5 Numerical Results

In the next series of panels we present the correlations as functions of the longitudinal variable  $x$ , for fixed points  $y_1 = 0.7, y_2 = 0.4$ , for increasing values of the elastic parameter  $\alpha$ .

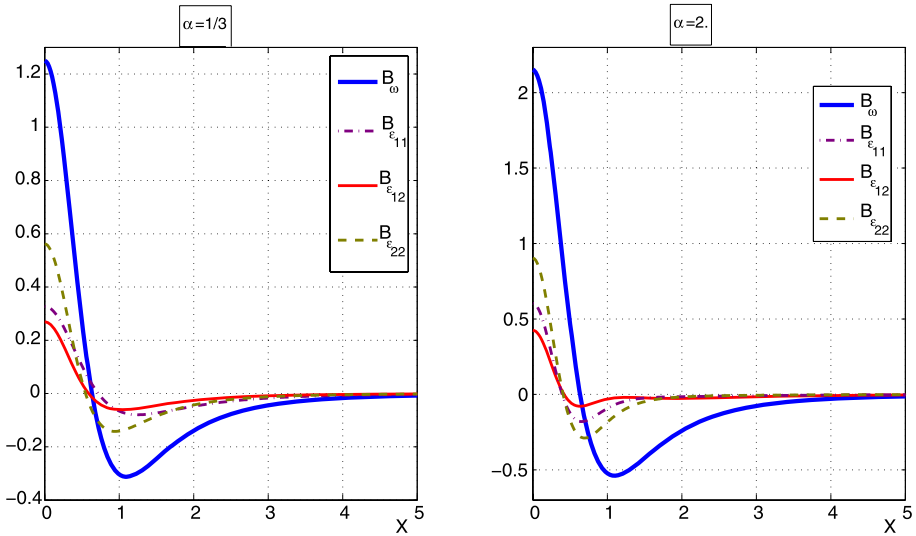


**Fig. 1** (Color online) The correlation functions  $B_\omega$ ,  $B_{\epsilon_{11}}$ ,  $B_{\epsilon_{12}}$ , and  $B_{\epsilon_{22}}$  for  $\alpha = 1/3$  (left panel), and  $\alpha = 2$  (right panel),  $y_1 = 0.7$ ,  $y_2 = 0.4$

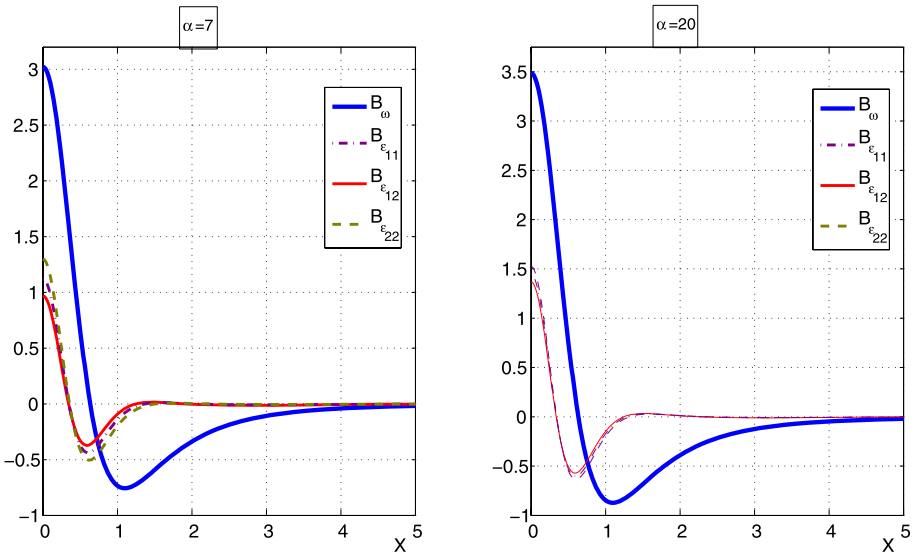


**Fig. 2** (Color online) The same as in Fig. 1, but for  $\alpha = 7$  (left panel), and  $\alpha = 20$  (right panel)

In Fig. 1, left panel, we plot the vorticity correlation function  $B_\omega$ , and the strain correlation function  $B_{\epsilon_{ij}}$  versus the coordinate  $x$ , for  $\alpha = 1/3$ , for fixed  $y_1, y_2$ . In the right panel of Fig. 1 we present the same curves but for  $\alpha = 2$ . It is seen that the fluctuation intensities are considerably increased. The impact of the further increase of the elasticity parameter  $\alpha$  on the correlation functions is shown in Fig. 2. It is clearly seen that the larger the value of  $\alpha$ , the higher the fluctuation intensities. However after this parameter reaches the value 20, the

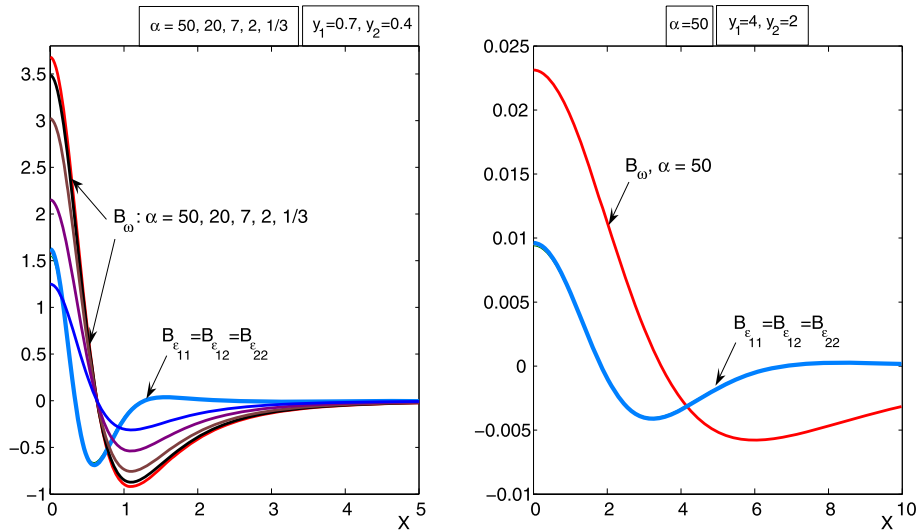


**Fig. 3** (Color online) The correlation functions  $B_\omega$ ,  $B_{\epsilon_{11}}$ ,  $B_{\epsilon_{12}}$ , and  $B_{\epsilon_{22}}$  for  $\alpha = 1/3, 2, 7, 20$  and  $50$  (left panel), and  $y_1 = 0.7, y_2 = 0.4$ . Right panel: illustrating the decrease of fluctuation intensity and increase of the correlation length, as  $y$  increases ( $y_1 = 0.7, y_2 = 0.4$ )

curves rapidly converge to some stable functions not depending on  $\alpha$ . Indeed, when  $\alpha > 50$  the calculation results for  $B_\omega$  converge to the upper curve shown in Fig. 3 (left panel). Here we show also the correlation functions  $B_{\epsilon_{11}}, B_{\epsilon_{12}}$ , and  $B_{\epsilon_{22}}$  for  $\alpha = 50$ . It is seen that these three functions are practically coincident. This can be explained as follows. Note that the case  $\alpha = \infty$  corresponds to the case of the Stokes flow regime (see [16] for explanation). The calculations show that beginning from  $\alpha = 50$ , we are practically in the Stokes regime. It can be shown that in this regime,  $B_{\epsilon_{11}} = B_{\epsilon_{12}} = B_{\epsilon_{22}}$ . This is seen also by comparing their partial spectral functions (16), (17), (18), and (19) at  $\alpha = \infty$ , which corresponds to  $\beta = 1$ . We show the limit curves at  $\alpha = 50$ , for  $y_1 = 4, y_2 = 2$  in Fig. 3, right panel.

To check both the derived formulae for the correlation functions and the K-L expansions we have made comparative calculations with different  $k$ , the number of the Fourier harmonics. Typical results of such calculations are given in the Fig. 4. In the left panel, the Monte Carlo error was less than 0.1% in the region of large and moderate small correlations, when choosing  $R = 300$ , and the number of harmonics  $n = 200$ . For small correlation values (less than 5%), the error was about 1%. In the right panel of Fig. 4, we illustrate the convergence rate of the Karhunen-Loève expansion. Here we compare the calculations of  $B_\omega$  for  $k = 50, 75$ , and  $k = 100$  with the exact result. It is seen that in this case, a 1%-error was achieved for  $k = 100$ . Note that for the mean energy  $\langle E(0, y) \rangle$  plotted versus the transverse coordinate  $y$  in the left panel of Fig. 5, the number of terms needed to achieve the error of 1% was larger, approximately,  $k \sim 600 - 700$ . This can be explained by the fact that close to  $y = 0$ , the mean energy increases as  $\sim y^{-3}$ .

The dependence of the vorticity correlation function on the transverse coordinate  $y$  (fixed  $y_1$ , varying  $y = y_2$ ) is shown in the right panel of the Fig. 5. It is clearly seen that with the depth, i.e., when  $y_2$  increases, the fluctuation intensities are rapidly decreasing while the correlation length is increasing.

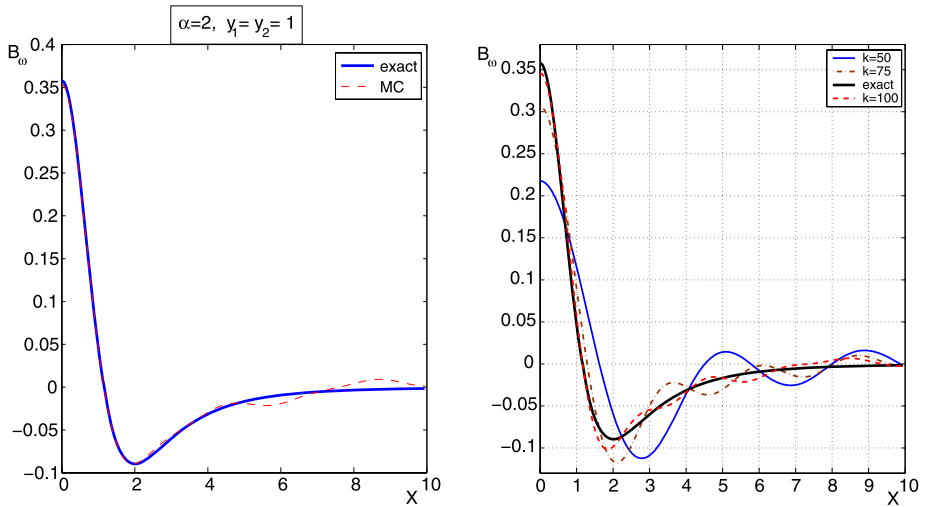


**Fig. 4** (Color online) Comparison of the Monte Carlo simulations (MC) against the exact result for the case of white noise boundary excitations, for the vorticity correlation function  $B_\omega$  (left panel). The convergence of K-L expansion is illustrated in the right panel, where  $B_\omega$  is shown for different numbers of harmonics

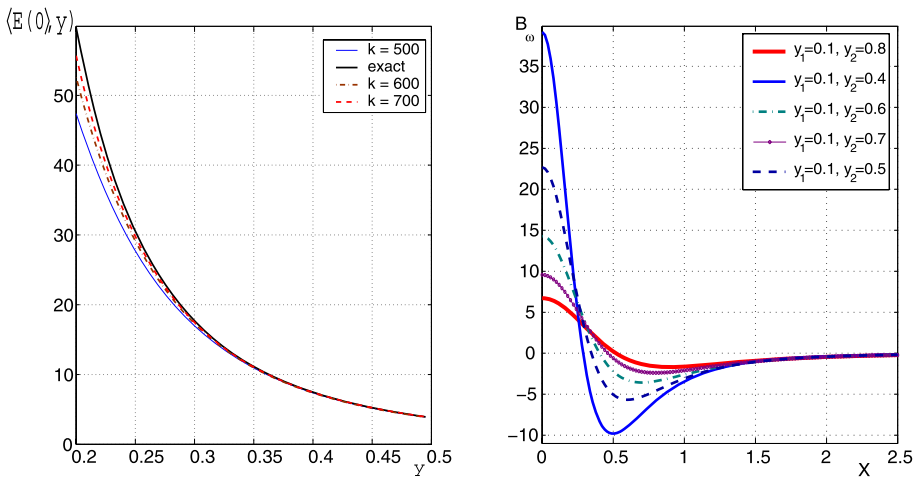


**Fig. 5** (Color online) Comparison of the Monte Carlo simulations (MC) against the exact result for the mean deformation energy (left panel), for different numbers of harmonics. The correlation function  $B_\omega(x)$  for different values of  $y_2$ , while fixed  $y_1 = 0.1$  is shown in the right panel, at  $\alpha = 50$

**Appendix: Some Fourier Transform Formulae**

We use the notation  $g(\tau, y) = F[h](\tau, y)$  for the Fourier transform of a function  $h(\xi, y)$  with respect to its first variable  $\xi$ , and  $F^{-1}[g](\xi, y)$  for its inverse:

$$F[h](\tau, y) = \frac{1}{2\pi} \int_{-\infty}^{\infty} e^{i\tau\xi} h(\xi, y) d\xi, \quad F^{-1}[g](\xi, y) = \int_{-\infty}^{\infty} e^{-i\tau\xi} g(\tau, y) d\tau.$$

We use the following simple property of the Fourier transform

$$\begin{aligned} F^{-1}[D_{\tau}^m g(\tau, y)] &= (i\xi)^m F^{-1}[g](\xi, y), \\ F^{-1}[D_y^m g(\tau, y)] &= D_y^m F^{-1}[g](\xi, y). \end{aligned} \quad (29)$$

The next list of Fourier transforms we used in the paper can be found in [5], and extended by using the property (29):

$$\begin{aligned} F^{-1}\left[\frac{y}{\pi(\tau^2 + y^2)}\right] &= e^{-|\xi|y}, \\ F^{-1}\left[\frac{\tau^2 - y^2}{\pi(\tau^2 + y^2)^2}\right] &= F^{-1}\left[\frac{\partial}{\partial y}\left(\frac{y}{\pi(\tau^2 + y^2)}\right)\right] = -|\xi|e^{-|\xi|y}, \\ F^{-1}\left[\frac{-2\tau y}{\pi(\tau^2 + y^2)^2}\right] &= F^{-1}\left[\frac{\partial}{\partial \tau}\left(\frac{y}{\pi(\tau^2 + y^2)}\right)\right] = i\xi e^{-|\xi|y}, \\ F^{-1}\left[\frac{2y(y^2 - 3\tau^2)}{\pi(\tau^2 + y^2)^3}\right] &= F^{-1}\left[\frac{\partial^2}{\partial y^2}\left(\frac{y}{\pi(\tau^2 + y^2)}\right)\right] = \xi^2 e^{-|\xi|y}, \\ F^{-1}\left[\frac{2\tau(3y^2 - \tau^2)}{\pi(\tau^2 + y^2)^3}\right] &= F^{-1}\left[\frac{\partial^2}{\partial y \partial \tau}\left(\frac{y}{\pi(\tau^2 + y^2)}\right)\right] = -i\xi|\xi|e^{-|\xi|y}, \end{aligned} \quad (30)$$

and

$$\begin{aligned} F^{-1}\left[\frac{6(y^4 + \tau^4 - 6y^2\tau^2)}{\pi(\tau^2 + y^2)^4}\right] &= -F^{-1}\left[\frac{\partial^3}{\partial y^3}\left(\frac{y}{\pi(\tau^2 + y^2)}\right)\right] = |\xi|^3 e^{-|\xi|y}, \\ F^{-1}\left[\frac{24y(y^4 + 5\tau^4 - 10y^2\tau^2)}{\pi(\tau^2 + y^2)^5}\right] &= F^{-1}\left[\frac{\partial^4}{\partial y^4}\left(\frac{y}{\pi(\tau^2 + y^2)}\right)\right] = |\xi|^4 e^{-|\xi|y}. \end{aligned}$$

## References

1. Dagan, G.: Flow and Transport in Porous Formations. Springer, Berlin (1989)
2. Farrell, B.F., Ioannou, P.J.: Stochastic forcing of the linearized Navier-Stokes equations. *Phys. Fluids A* **5**(N11), 2600–2609 (1993)
3. Ghanem, R.G., Spanos, P.D.: Stochastic Finite Elements. A Spectral Approach. Courier Dover, New York (2003)
4. Giordano, A., Uhrig, M.: Human face recognition technology using the Karhunen-Loeve expansion technique. Regis University, Denver, Colorado. <http://www.rose-hulman.edu/mathjournal/archives/2006/vol7-n1/paper11/v7n1-11pd.pdf>
5. Gradshteyn, I.S., Rygik, I.M.: Tables of Integrals, Sums, Series and Products. Nauka, Moscow (1971) (in Russian)
6. Kaipio, J., Kolehmainen, V., Somersalo, E., Vauhkonen, M.: Statistical inversion and Monte Carlo sampling methods in electrical impedance tomography. *Inverse Probl.* **16**, 1487–1522 (2000)
7. Kramer, P., Kurbanmuradov, O., Sabelfeld, K.: Comparative analysis of multiscale Gaussian random field simulation algorithms. *J. Comput. Phys.* **226**, 897–924 (2007)
8. Lucor, D., Su, C.H., Karniadakis, G.E.: Karhunen-Loeve representation of periodic second-order autoregressive processes. In: International Conference on Computational Science, pp. 827–834. Springer, Berlin (2004)
9. Monin, A.S., Yaglom, A.M.: Statistical Fluid Mechanics: Mechanics of Turbulence, vol. 2. MIT Press, Cambridge (1981)
10. Pahir, J., Alam, S., Garra, B., et al.: Elastography: Imaging the elastic properties of soft tissues with ultrasound. *J. Med. Ultrason.* **29**, 155–171 (2002)



11. Phoon, K.K., Huang, W.H., Quek, S.T.: Simulation of strongly non-Gaussian processes using Karhunen-Loeve expansion. *Probab. Eng. Mech.* **20**, 188–198 (2005)
12. Rozanov, Yu.A., Sanso, F.: The analysis of the Neumann and the oblique derivative problem: the theory of regularization and its stochastic version. *J. Geod.* **75**, 391–398 (2001)
13. Sabelfeld, K.K.: *Monte Carlo Methods in Boundary Value Problems*. Springer, Berlin (1991)
14. Sabelfeld, K.K.: Expansion of random boundary excitations for elliptic PDEs. *Monte Carlo Methods Appl.* **13**(N5–6), 405–453 (2007)
15. Sabelfeld, K.K.: Evaluation of elastic coefficients from the correlation and spectral tensors in respond to boundary random excitations. In: *Proc. Int. Conference on Inverse and Ill-Posed Problems of Mathematical Physics. Dedicated to Professor M.M. Lavrentiev on Occasion of his 75-th Birthday*. Novosibirsk, 21–24 August 2007
16. Sabelfeld, K.K.: Stokes flows under random boundary velocity excitations. *J. Stat. Phys.* **133**(N6), 1107–1136 (2008)
17. Sabelfeld, K., Shalimova, I.A.: Elastic half-plane under random displacement excitations on the boundary. *J. Stat. Phys.* **132**(N6), 1071–1095 (2008)
18. Shinozuka, M.: Simulation of multivariate and multidimensional random processes. *J. Acoust. Soc. Am.* **49**, 357–368 (1971)
19. Sowers, R.B.: Multidimensional reaction-diffusion equation with white-noise boundary perturbations. *Ann. Probab.* **22**(N4), 2071–2121 (1994)
20. Van Trees, H.L.: *Detection, Estimation and Modulation Theory, Parts 1–3*. Wiley, New York (1968)
21. Xiu, D., Shen, J.: An efficient spectral method for acoustic scattering from rough surfaces. *Commun. Comput. Phys.* **2**(N1), 54–72 (2007)
22. Frank Xu, X.: A multiscale stochastic finite element method on elliptic problems involving uncertainties. *Comput. Methods Appl. Mech. Eng.* **196**(25–28), 2723–2736 (2007)
23. Yaglom, A.M.: *Correlation Theory of Stationary and Related Random Functions I. Basic Results*. Springer, Berlin (1987)